

The challenges of gas-cooled reactor technology for space propulsion and the development of the JANUS space reactor concept

Aiden Peakman^a, Robert Gregg^a

^a*National Nuclear Laboratory, Chadwick House, Warrington, WA3 6AE*

Abstract

There is a strong motivation to develop high-power output nuclear fission reactors (around 1 MWe) for space applications, such as high-payload missions and long-duration missions beyond Mars, where the reduced solar flux makes using alternative energy sources challenging. Many published gas-cooled reactor designs for space applications deliver outputs in the 100 kWe regime, with typical power densities of around 4 MW/m³. Here we present a gas-cooled reactor design – referred to as JANUS – employing He-Xe coolant and operating on a direct Brayton cycle, that can achieve a high power output (around 0.8 MWe) and higher power density (24 MW/m³) than previously published designs. The core employs a coated particle fuel form with uranium nitride kernels in a graphite matrix and with a high packing fraction (45%).

Starting from the CEA's published OPUS space reactor design, a variety of approaches were considered for achieving high power densities in a gas-cooled reactor, including changing the core aspect ratio. Our JANUS design uses a decreased coolant channel diameter and fuel element pitch, whilst increasing the number of fuel elements and employing radial enrichment zoning. The design achieves a significant increase in power density whilst obeying core-life limits of 2000 Effective Full Power Days and a peak fuel operating temperature of 1900 K. The core has been modelled neutronicly with the ERANOS and SERPENT codes, with a simple yet robust thermal dimensioning tool developed by us to study peak fuel temperatures, to ensure the fuel operates within its design limitations and to aid optimisation.

Keywords: Nuclear reactors, Space propulsion, Space power, BISO fuel, ERANOS, Uranium Nitride

1. Introduction

Most interplanetary missions rely on either solar power or decay heat from radioactive sources using radioisotope thermoelectric generators (RTGs) for electricity production (Launius, 2008). However, in order to generate sufficient power for a large mission payload, especially for long-duration missions beyond Mars, the role of a conventional nuclear reactor

Email address: aiden.w.peakman@uknpl.com (Aiden Peakman)

becomes more apparent. This is a result of reduced solar flux beyond Mars and the low power densities possible using alternative solutions. In addition, there is desire to employ electrical propulsion for long duration missions due to the improved fuel efficiency and reliability offered by ion-propulsion (Noca and Polk, 2002, NASA, 2004, European Science Foundation, 2014). To deliver electricity for onboard systems including electrical propulsion, a relatively high electrical output of around 1 MWe is required for the following mission types (European Science Foundation, 2014):

- Near Earth Orbiter (NEO) deflection: a hypothetical mission to deflect large asteroids capable of threatening life on Earth by acting as a gravity tractor
- Outer Solar System missions with large mission payloads between 3 to 10 tonnes
- Lunar orbit tug: a space vehicle capable of transferring heavy mission payloads from low earth to high earth orbit
- Cargo support for a manned Mars mission

For relatively large electrical outputs, a high core outlet temperature (around 1300 K (Lokhov, 2009)) is also necessary to reduce launch mass and volume by enhancing thermal efficiency and ensuring the radiator size required to reject heat to space is minimised. Furthermore, to ensure the reactor design is available in the short to medium term, reliance on previous conceptual designs and tested materials is essential. For all of the above applications, there will be no human contact during operation. Therefore, in the case of a nuclear reactor being employed to power such missions, the normal criteria relating to minimising dose to humans and the environment will not be an overriding priority.

The objective of this study was to adapt an existing reactor design to target the above applications. Therefore the reactor design must generate a sufficiently high electrical output whilst optimising both core mass and volume. Furthermore, the trade-off between increasing core power density and impacts on systems outside the core region, for example the power conversion technology are considered.

There have already been several large programmes creating conceptual closed thermal cycle nuclear energy systems with high core outlet temperatures (around 1300 K) and moderate to high electrical outputs (around 100 kWe or more). Table 1 summarises a number of key space reactor power systems including: those operating at moderate to high electrical outputs (ERATO, FBR, the nominal OPUS concept, NPPU and SP-100); those that employ gas coolants (FBR, the nominal OPUS concept and NPPU); some of the historic designs that were launched (Topaz-1 and SNAP-10A) or extensively tested (Topaz-2); and some of the more modern designs (HOMER, KRUSTY and SAFE-400).

Historically, many space reactor designs, and also some modern designs, have employed Highly Enriched Uranium (HEU) fuel, with a number of designs employing fuel enriched above 90 wt.% such as TOPAZ, SNAP-10A and KRUSTY (El-Genk and Tournier, 2004, WNA, 2020). Some reactor designs have used Low Enriched Uranium (LEU) fuel; however, there is an inherent trade-off with such designs: for the same power and length of reactor operation, the use of LEU fuel makes the reactor heavier and larger in dimension, resulting in significantly lower power densities (Lee et al., 2015). Hence, for long duration missions

Table 1. Summary of space reactor power systems

Reactor	Country	Coolant	Fuel	Spectrum	Power	Reference(s)
ERATO	France	Li	UN	Fast	0.02 - 0.2 MWe	Carre et al. (1987), Delaplace (1987)
FBR	USA	He	UO ₂	Thermal	> 10 MWe	Pierce (1984), Botts et al. (1984)
HOMER	USA	Na	UO ₂	Fast	0.02 MWe	Poston (2000)
KRUSTY	USA	Na	U-Mo	Fast	0.001 - 0.01 MWe	WNA (2020), Briggs et al. (2018)
Nominal OPUS concept	France	He-Xe	UO ₂	Fast	0.1 MWe	Raepsaet and Pascal (2007), Likhov (2009)
NPPU	Russia	He-Xe	Unknown	Unknown	1 MWe	OSNET (2014)
SAFE-400	USA	Na	UN	Fast	0.1 MWe	WNA (2020)
SNAP-10A	USA	NaK	U-ZrH _x	Thermal	< 0.001 MWe	WNA (2020)
SP-100	USA	Li	UN	Fast	0.1 MWe	Demuth (2003), NASA (2005), Brandon and Sapir (1986)
Topaz-1	Russia	NaK	UO ₂	Thermal	0.005 - 0.01 MWe	WNA (2020)
Topaz-2	USA/Russia	NaK	UO ₂	Thermal	0.006 MWe	Polansky and Houts (1995)

and higher power outputs HEU fuel has been the preferred choice (Khandaq et al., 2020). Nevertheless, the obstacles with using HEU fuel should not be ignored, there will be additional security measures and associated costs with using HEU fuel (Nam et al., 2016). The motivation for a high-power density, long-life system in this study results in the use of HEU material. The fuel enrichments studied here range between 20 and 90 wt.%, noting that the original OPUS design employed fuel enriched to 93 wt.% (Raepsaet and Pascal, 2007, Likhov, 2009).

For terrestrial based energy systems employing gas-coolant, helium is the preferred coolant due to its high heat transfer coefficient (Peakman et al., 2018). However, lighter coolants (such as He) result in high aerodynamic loading on the compressor, thereby requiring either a higher rotational speed or larger impeller size to compensate (El-Genk and Tournier, 2006). The higher rotational speed or larger impeller size result in larger turbo-machinery and hence additional weight and/or volume. Therefore, for space applications, there is a compromise between choosing a coolant with a sufficiently high heat transfer coefficient and a heavier gaseous coolant (such as Xe). Therefore, a He-Xe mixture is preferred for space applications (El-Genk and Tournier, 2006).

In this study, the nominal French OPUS design (0.1 MWe) was taken as a starting point, with this design chosen for further optimisation and investigation because:

- this core concept was considered to have the largest potential for optimisation;
- the concept can operate at the high outlet temperatures required due to the use of a gaseous coolant and the selected materials (1300 K); and
- the details of this concept are well documented in the open literature.

The key aims were to develop a space reactor with high-power output (around 1 MWe) and significantly higher power density than previous published gas-cooled reactor designs, which are in the 100 kWe range. Table 2 summarises the key core parameters that the design in this study must meet. To ensure the launch mass and volume are minimised, several core optimisations have been proposed in this study to increase power density. A reduction in core volume will have neutronic and thermal implications, both of which have been modelled using the methods and modifications outlined in Section 2. The modifications include: core geometry and fuel element changes necessary to enhance heat transfer from the graphite surface resulting in an increased power density; and radial enrichment zoning which has also

been incorporated into the design to flatten the power profile across the core, leading to a reduction in peak operating temperature and a subsequent up-rate in power density.

Table 2. Key core parameters for the space reactor iterations

Parameter	Value	Reference(s)
Effective Full Power Days Operation	2000 days	Raepsaet and Pascal (2007)
Beginning of life excess reactivity	3000 pcm	Raepsaet and Pascal (2007)
Peak Fuel Temperature	1900 K	IAEA (2010), Lokhov (2009)
Inlet Temperature	880 K	Lokhov (2009)
Outlet Temperature	1300 K	Lokhov (2009)

2. Method

The method for designing suitable updated reactor concepts starting from the nominal OPUS design was based on an iterative approach between neutronic modelling, using ERANOS 2.0 (see Section 2.2), and thermal-hydraulic performance using the thermal dimensioning tool outlined in Section 2.3. At all points in the iterative process, the designs were screened against the key parameters highlighted in Table 2.

2.1. The nominal OPUS core concept

The OPUS reactor concept (Raepsaet and Pascal, 2007) is a gas-cooled fast reactor developed by CEA (see Figure 1). It is designed to cover a wide range of power outputs (100 to 500 kWe). However, it is only the 100 kWe variant that is described in sufficient detail in the open literature to develop a model of the core. No information was found on the thermal output of the 100 kWe system but based on the specific heat capacity (C_p) for coolant employed in OPUS design (which was 244.54 J/kg/K), the temperature rise across the core (ΔT), which was 420 K and the reported mass flow rate (\dot{m}), which was 3.6 kg/s (Lokhov, 2009), the thermal output is estimated to be around 370 kWth using Equation 1.

$$\dot{Q} = \Delta T \dot{m} C_p \quad (1)$$

where \dot{Q} is the rate of change of energy. Hence the thermal efficiency is determined to be 27%.

The original core design contains 252 hexagonal fuel elements arranged to form the core cylinder. The core itself comprises 4 individual core quadrants. These are designed to separate in the event of launch failure in order to reduce the risk of inadvertent criticality if immersed in clay or water. A He-Xe coolant mix at a core inlet temperature of 880 K with an atomic mass of 85 g/mol enters the top of the core vessel, cooling the reactor pressure vessel. The He-Xe gas enters the bottom of the core and flows through coolant channels centrally located in every hexagonal fuel element. Ultimately, the coolant leaves the core with an average outlet temperature of 1300 K, driving a direct cycle Brayton engine. Direct cycle Brayton engines are the preferred energy conversion option for space reactor

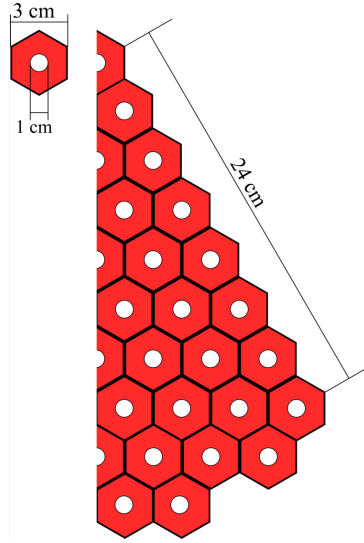


Fig. 1. The nominal OPUS core layout

propulsion in the range 0.1 MWe to 10's MWe since they allow for compact and low specific mass (kg/MWe) turbo-machinery, thereby aiding in reducing launch mass (El-Genk and Tournier, 2006). The key parameters of the CEA original OPUS concept are summarised in Table 3.

The fuel elements in the nominal OPUS concept have a hexagonal pitch of 3 cm with a central 1 cm diameter coolant channel. The fuel comprises a graphite matrix with 45% (by volume) bistructural isotropic (BISO) fuel particles (Raepsaet and Pascal, 2007). The kernels are UO_2 and enriched to 93 wt.%.

Table 3. Nominal OPUS core key parameters (Raepsaet and Pascal, 2007, Lokhov, 2009).

Parameter	Nominal OPUS Core
Thermal power	0.370 MWth
Electrical power	0.100 MWe
Active core diameter	48 cm
Active core height	48 cm
^{235}U enrichment	93 wt.%
Fuel element pitch (across flats)	3 cm
Coolant channel diameter	1cm
Fuel elements in core	252
Kernel type	UO_2
Coolant type	85 g/mol He-Xe
Coolant flow rate	3.6 kg/s
Radial reflector thickness	8 cm
Axial reflector	8 cm

Note that the fuel employed in the reactor design developed here is the same type of BISO fuel that is proposed in the nominal OPUS design but with a uranium nitride (UN) kernel, as discussed in Section 2.3.3. BISO fuel was the first demonstrated successful coating technology with the name referring to the two material components (the fuel kernel and the PyC) and their isotopic geometries (IAEA, 2010, Howard et al., 1978). Further developments in coated particle fuel resulted in an additional layer of silicon carbide (SiC) and resulted in the so-called TRISO (tristructural isotropic) fuel concept (IAEA, 2010, Howard et al., 1978). The purpose of the additional SiC is to provide a high degree of mechanical and thermal resistance. Moreover, the SiC layer acts as a leak tight seal around the previous layers and is particularly good at retaining the metallic fission products and tritium (IRSN, 2015, Sawa, 2012, Verfondern, 2012). Table 4 provides a comparison between conventional TRISO fuel in modern High Temperature Reactor (HTR) designs and the BISO fuel employed in the OPUS and JANUS concepts studied here. It is important to note that in conventional TRISO fuel the kernel constitutes around 35% of the total particle volume, whereas in the BISO particles used in this study the kernel make up around 70% of the total particle volume. Therefore, with the BISO fuel concept, for a given packing fraction, there is a greater concentration of fissile material present in the core. Hence, whilst BISO fuel has been superseded in many applications by TRISO fuel, BISO fuel is still a popular choice for space reactors due to the higher volume fraction of fissile material (Raepsaet and Pascal, 2007, Lokhov, 2009). The higher fuel volume fraction is important when a compact and light-weight core design is required.

Table 4. Comparison between conventional TRISO particles (Petti et al., 2012) and OPUS/JANUS BISO particles (Raepsaet and Pascal, 2007)

Layer	TRISO	BISO
UO ₂ kernel radius	500 μm	820 μm
Porous carbon thickness	90 μm	45 μm
Inner Pyrolytic Carbon thickness	40 μm	-
SiC thickness	40 μm	-
Outer Pyrolytic Carbon thickness	40 μm	45 μm

As noted, the drawback of adopting BISO fuel is the increased likelihood of fission product release relative to TRISO particles (Gulden et al., 1977, Petti et al., 2012). However, given that the reactor core will begin operation only once launch is complete (Bennett, 2002) and unmanned missions are considered, as outlined in Section 1, the higher fission product release can be tolerated.

The volumetric packing fractions in the OPUS designs and variants considered here are 45%. This is high by historical standards (with many HTR systems having packing fractions less than 35% (Petti and Maki, 2005)); however, packing fractions up to 50% have been considered for prismatic fuel designs (Petti, 2007). There is general agreement that high packing fractions in prismatic designs result in an increased likelihood of fuel failure (Petti, 2007). It should be noted that whilst an increased likelihood of fission product release can be tolerated, given the overriding priority of a light-weight design, it is important that

steps are taken to minimise fission product release where possible. This is because the high operating temperatures of the core and targeted long core-life mean that in the presence of a large release of chemically aggressive fission products, this could result in failure of components within the reactor or turbo-machinery.

The fuel particles considered here have 800 μm fuel kernel diameter and 100 μm combined thickness of porous and pyrolytic carbon (Kingrey, 2003), hence each particle was around 1 mm in diameter. Note that particulate fuel typically has kernel diameters of around 500 μm , with some limited experience with 800 μm fuel kernels (Simon and Capp, 2002).

For the nominal OPUS core, reactivity during normal operation is controlled by 12 external reflector vertically hinged shutters (Raepsaet and Pascal, 2007). By opening the shutters, neutron leakage can be varied, which for such a small core significantly impacts overall core reactivity. Under operational conditions and with all shutters closed, $k\text{-eff}$ would be 1.04. With all shutters open, $k\text{-eff}$ would be 0.94 (Lokhov, 2009).

2.2. Neutronic modelling

The BISTRO module within the ERANOS 2.0 code suite (Rimpault and Grimstone, 2002) was used in conjunction with the JEF-2.2 Nuclear Data Library (NEA, 2000) to model an R-Z representation of the core, reactor pressure vessel (RPV) and surrounding reflector regions ¹. In all ERANOS calculations the individual fuel elements (comprising central coolant channels, graphite and particle fuel) were modelled homogeneously. Furthermore, consistent with other Gas-cooled Fast Reactor studies (Ponya and Czifrus, 2017, Da Cruz et al., 2006), the fuel elements were modelled isothermally, but in this case with a temperature of 1580 K.

Initially, there was some concern over homogenising the fuel elements at the start of the calculation sequence and that using an R-Z representation of the core in subsequent calculations would introduce a large discrepancy. In addition, the use of ERANOS (a fast reactor code) to model a system that contains a significant amount of graphite and beryllium, and would be expected to have a softer spectrum than a typical fast reactor, also raised concerns around the validity of the approach adopted. Therefore, confirmatory Monte Carlo calculations were performed using SERPENT-2 (2.1.23) with the JEF-2.2 Nuclear Data Library (Leppanen, 2007) to highlight the impact of homogenising the core design, as well as to validate the ERANOS calculation route. For the purposes of this confirmatory calculation, fuel temperatures of 1500 K were used in both the ERANOS and SERPENT calculations. It should be noted that SERPENT has cross-sections tabulated at specific temperatures (300 K, 600 K, 900 K, 1200 K and 1500 K). Note that the spectrum for the final core iteration developed in this study is included in Section 3.4.

The results shown in Table 5 indicate that homogenising the core has a relatively small impact on core reactivity (366 pcm). Furthermore, a difference of 654 pcm between the homogenous ERANOS calculation and a higher fidelity heterogeneous SERPENT calculation suggests the method used is sufficiently accurate for a scoping analysis of this nature.

¹Whilst ERANOS 2.3 with JEFF-3.1 Nuclear Data Library could be considered state-of-the-art, for the purpose of this scoping study ERANOS 2.0 with JEF-2.2 is considered acceptable.

Table 5. Reactivity difference between the homogeneous ERANOS model and the different SERPENT configurations

SERPENT Configuration	Reactivity difference
Homogeneous	288 ± 1 pcm
Heterogenous	654 ± 1 pcm

The ERANOS model was used to assess the enrichments required in the core to maintain sufficient reactivity for at least 2000 effective full power days, and to develop radial enrichment zoning patterns that minimise power peaking throughout core life. However, in order to predict peak temperatures in the core, and in doing so determine the size of the core, a bespoke thermal dimensioning computer code was developed. The code used fundamental heat transfer theory (Incropera and DeWitt, 1990) to quickly assess conditions in the coolant, graphite surface, through the graphite block and within the fuel particle itself, as outlined in the following section.

2.3. Thermal dimensioning tool

The calculation sequence (summarised in Figure 2) for determining the peak temperature (T_{peak}) starts with determining the bulk temperature (T_{bulk}) of the coolant, then the temperature at the surface of the fuel element ($r = r_{\text{surf}}$) - where fuel element refers to the individual hexagonal structure with a central coolant channel and graphite matrix with fuel particles inside (see Figure 2). To simplify the method, the hexagonal fuel element has been modelled as a cylinder with the same cross sectional area. In actual fact, the temperature at the corner of the hexagonal fuel assembly will be slightly higher since the distance from the coolant channel will be greater than that of the cylindrical radius. However, as adiabatic boundary conditions have also been assumed, this will likely counteract this non-conservative assumption.

The calculation is followed by determining the temperature at the outer surface of the fuel element $r = R_1$ and finally the peak temperature, which is determined at the temperature at the centre of a fuel particle that neighbours the surface $r = R_1$. This process is captured in the thermal dimensioning tool, which for a particular core configuration can determine T_{peak} and was developed as part of this study.

The thermal dimensioning tool works on the following basis:

- The temperature increase along the fuel element is determined using the power in each R-Z zone from the ERANOS model, along with the specific heat capacity and an estimate for the mass flow rate, to allow for the bulk coolant temperature at any location to be determined. The heat capacity employed for the nominal Xe-He coolant mixture was 20.8 J/mole/K (El-Genk and Tournier, 2006).
- Calculating the radial temperature increase from the bulk coolant to the surface of the graphite block as detailed in Section 2.3.1.

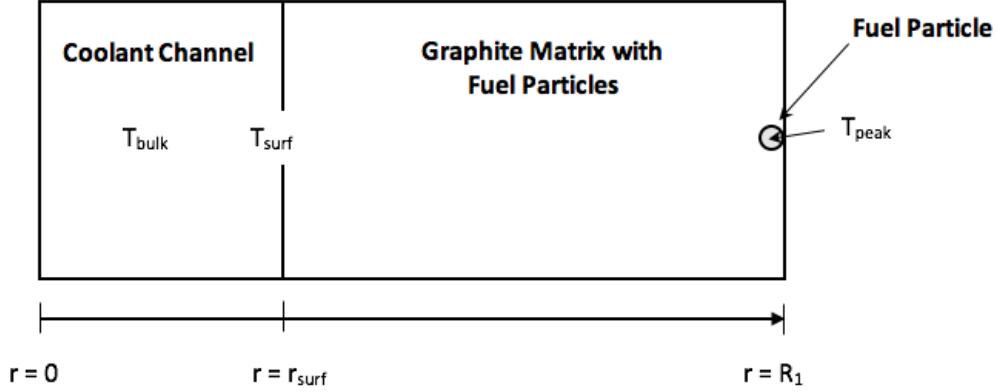


Fig. 2. Defined temperature regions within a particular axial zone, including the peak temperature (T_{peak}) which is at the centre of fuel particle (not to scale) neighbouring the fuel element outer surface at $r = R_1$. The centre of the coolant channel is located at $r = 0$.

- Calculating the radial temperature profile from the graphite surface to the fuel element outer surface as detailed in Section 2.3.2.
- Calculating the temperature of a fuel kernel in closest proximity to the fuel element outer surface as detailed in Section 2.3.3.

2.3.1. Temperature increase from bulk coolant to the surface of the graphite block

Starting with Equation 2 for the heat transfer rate per unit area (W/m^2):

$$q'' = h(T_{\text{surf}} - T_{\text{bulk}}) \quad (2)$$

where h is the heat transfer coefficient, and T_{surf} and T_{bulk} are the temperatures at the positions shown in Figure 2. The heat transfer coefficient is given by

$$h = \frac{k_{\text{mix}} \times N_u}{D_H} \quad (3)$$

where k_{mix} is the thermal conductivity of the particular coolant mixture, N_u is the Nusselt number, which in this study it is determined through the Kays correlation (Reid et al., 2007), and D_H is the equivalent diameter.

Rearranging Equation 2 gives:

$$T_{\text{surf}} = T_{\text{bulk}} + \frac{q''}{h} \quad (4)$$

where the heat transfer rate per unit area can be determined for a particular axial zone using the heat surface area and the power produced in each R-Z mesh from ERANOS.

2.3.2. Temperature increase from the graphite surface to the fuel element outer surface

Starting from the cylindrical form of the heat balance equation (Incropera and DeWitt, 1990) and assuming: 1) steady-state conditions; and 2) that thermal energy will primarily flow in the radial direction, the cylindrical form of the heat balance equation becomes:

$$\frac{1}{r} \frac{\partial (kr \frac{\partial T}{\partial r})}{\partial r} = -\dot{q} \quad (5)$$

where \dot{q} is the energy generation per unit volume in the graphite block of the fuel element (W/m^3), which is again determined using the power density from ERANOS, r is the radial distance through the fuel element (m), k is the effective thermal conductivity of the graphite-fuel particle mixture ($\text{W}/\text{m}/\text{K}$) and T is the temperature (K). Note that the effective thermal conductivity within the graphite block (BISO fuel particles and graphite) is determined using Maxwell's method detailed in (Carslaw, 1959).

Assuming no significant variation in thermal conductivity as a function of radius and applying the following boundary conditions: at the fuel element outer radius (R_1) no heat transfer is assumed (i.e. an adiabatic boundary condition); and the fuel temperature at the inner radius (R_0) is given by T_{surf} , the temperature at a given radius within the graphite-fuel particle mixture is provided by Equation 6.

$$T = T_{\text{surf}} + \frac{\dot{q}}{2k} \left[\left(\frac{R_0^2 - R_1^2}{2} \right) + R_1^2 \ln \left(\frac{R_1}{R_0} \right) \right] \quad (6)$$

2.3.3. Temperature increase across a coated particle located on the fuel element outer surface

The radial temperature distribution across the coated particle is determined via Fourier's Heat Equation and assuming the pyrolytic carbon thermal conductivity does not vary with radius, resulting in:

$$T(r) = T_0 + \frac{q}{4\pi k} \left(\frac{1}{r} - \frac{1}{R_0} \right) \quad (7)$$

where q is the total heat transfer rate from a single particle, k is the thermal conductivity across the carbon layer of interest, and R_0 relates to the radius at the boundary condition. T_0 and R_0 are initially set to the values relating the temperature and radius at the outer surface of the coated particle, respectively. $T(r)$ is used to calculate the radial temperature increase across the pyrolytic carbon layer and then, using this result as the new boundary condition (T_0), the temperature increase across the porous carbon layer is calculated.

Finally, using the heat balance equation in spherical coordinates, the temperature at the centre of the coated particle (i.e. when $r = 0$) is calculated via:

$$T(r = 0) = T_0 + \frac{\dot{q}t_{\text{kern}}}{6k} - \frac{\dot{q}r^2}{6k} \quad (8)$$

where \dot{q} is the energy per unit volume of an individual fuel kernel (determined using ERANOS), k is the thermal conductivity of the fuel kernel and t_{kern} is the kernel radius. The

boundary condition, T_0 , is determined using the previous calculation for the temperature increase across the porous carbon layer. According to (IAEA, 2008), the thermal conductivity at 1800 K for UN is 26.2 W/m/K. No data on irradiation degradation on thermal conductivity could be found so a lower value of 20 W/m/K was conservatively chosen. Note that as a consequence, the effective thermal conductivity of the fuel/graphite mix was calculated to be 20.44 W/m/K.

2.4. Thermal modelling

For all of the core iterations developed in this study, the R-Z ERANOS model comprised 100 radial and 13 axial zones making a total of 1300 equi-volume zones. The thermal power per zone was predicted by ERANOS and used by the thermal dimensioning tool outlined in Section 2.3 to predict operating temperatures. For each of the 100 annuli, a 13-zone coolant channel surrounded by a single fuel element was modelled with a zero heat flux (adiabatic) outside boundary condition. The thermal dimensioning tool was used to:

- predict the temperature increase axially along the fuel stack; and
- predict the temperature distribution radially from the bulk coolant, through the graphite-fuel matrix and a single fuel particle situated on the zero heat flux boundary.

A temperature distribution for the nominal OPUS core concept with a given coolant flow rate and prescribed inlet and outlet coolant temperatures is available from (Lokhov, 2009, Pascal, 2010). Using power densities from the ERANOS model of the nominal OPUS core developed in this study and the thermal dimensioning tool described above, the results from the thermal dimensioning tool was compared against the CEA results. The CEA thermal analysis employed the Cast3M finite element software package (Raepsaet and Pascal, 2007), which can provide temperature predictions of a higher accuracy than the thermal dimensioning tool developed in this study but with a higher computational cost. The code comparison was performed using the temperatures in the central fuel channel of the core where temperatures are highest and therefore most limiting. The results of the code comparison are shown in Figure 3

The error bars on the Cast3M results relate to the fact that Ref. (Raepsaet and Pascal, 2007) gives the temperature distribution in each axial zone within a range of ± 37.5 K. As Figure 3 shows, there is good agreement between thermal dimensioning tool and Cast3M. The code comparison performed between the TDT approach and Cast3M results shows that for determining peak temperatures the TDT approach is sufficient for the scoping and optimisation process undertaken in this study. However, some discrepancies would be expected between the TDT approach and Cast3M as a result of:

- The CEA calculation modelling irradiation induced graphite thermal conductivity degradation (the thermal dimensioning tool model assumes constant thermal conductivity throughout life); and
- the conservative simplifications: ignoring radiative heat transfer from the core periphery and the (adiabatic) boundary conditions used to calculate the temperature increase through each fuel element.

Furthermore, the relatively flat fuel temperature profile towards the top of the core is due to the continual increase in enthalpy increase along the coolant channel balancing the reduction in power density produced within the fuel from one axial zone to the next (see Figure 3). Towards the axial periphery of the core, the beryllium reflector will result in the reflection of more thermalised neutrons into the system, thereby resulting in elevated powers in these regions.

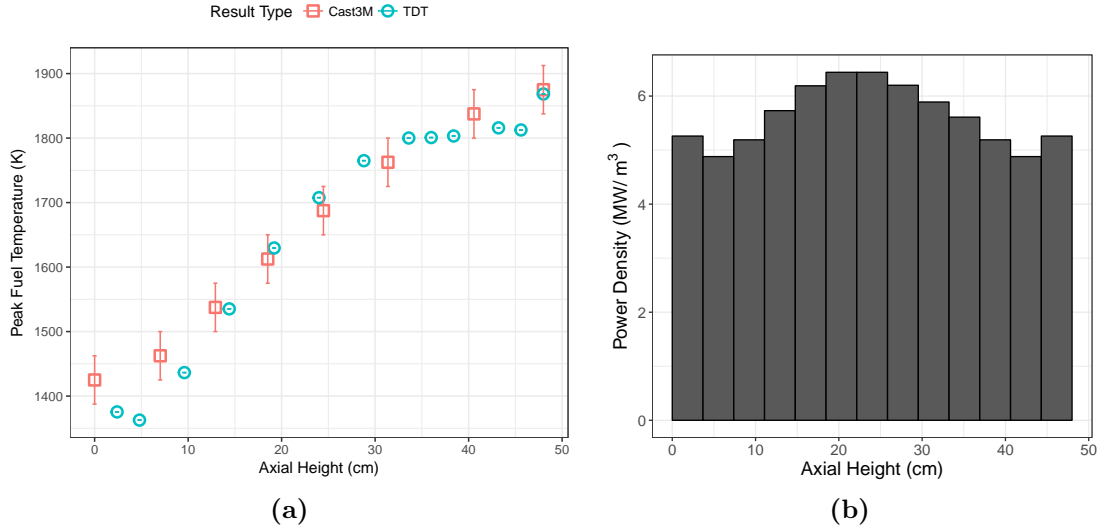


Fig. 3. Comparison of temperature distributions from CEA’s Cast3M finite element software and the Thermal Dimensioning Tool (TDT) developed as part of this study (left) and calculated power distribution in each axial zone from ERANOS (right)

3. Up-rating the nominal OPUS design

A key aim of this study was to develop a gas-cooled reactor for space applications (as outlined in Section 1) that can achieve electric power outputs close to 1 MWe. The nominal OPUS design already operates at close to the 1900 K summarised in Table 2, noting that the majority of the temperature increase from the bulk coolant to the peak fuel temperature is at the coolant channel surface. Hence, simply increasing the power output in the nominal core configuration will result in excessive temperature conditions. Therefore, all design variants included radial enrichment zoning, with between 4 and 5 radial zones chosen (noting that the the nominal OPUS core employed only a single radial enrichment) to keep the peak temperature below 1900 K. Furthermore, all core designs developed in this study implemented UN fuel kernels to reduce the fuel enrichment and allow greater flexibility in the range of radial enrichments to aid improvements in power profiles. An alternative approach, not studied here, would have been to keep the enrichment fixed at 93 wt.% and vary the packing fraction to simulate variations in fissile concentration.

It should be noted that whilst Refs. (IAEA, 2010, Likhov, 2009) indicate upper temperature limits on the 1900 K, experience with TRISO fuel operating at such high temperatures

is limited. German experience for conventional (UO_2) TRISO fuel found failure rates of 1.65×10^{-5} during heating tests up to 1900 K, with tests running for $\sim 10^2$ hours (Verfondern, 2012). Therefore, greater levels of testing would need to be performed to determine failure rates – noting that failure rates are highly temperature dependent and may require some trade-off between targetted power density and acceptable failure rates for the purpose of reactor design developed here.

Many UN studies assume isotopically pure ^{15}N fuel (between 95% and 99.9% ^{15}N content) due to the parasitic absorption of the predominant ^{14}N nuclide (which constitutes 99.6% of naturally occurring nitrogen, with remaining 0.4% being ^{15}N) and also the formation of radioactive ^{14}C during irradiation of ^{14}N , which represents a disposal concern (IAEA, 2019, Ray et al., 2012). In the analysis performed here, the UN fuel is modelled as 100% enriched ^{15}N . A comparison on the reactivity impact of employing 95% vs 100% ^{15}N is included in Section 3.4.

Note that the use of a high-density UN fuel operating at temperatures up to 1900 K in coated particle form would need to be validated. There currently appears to be limited to no experience with irradiation of UN coated fuel; however, UN coated particles have successfully been fabricated (Ledergerber et al., 1992, 1996, Ganguly, 1993). Overall, the extent of irradiation experience with UN is far lower than UO_2 under fast reactor conditions, with UN exhibiting low creep rates and high swelling rates, which may prove limiting for this design (Guerin, 2012). An experimental programme would be required to qualify the fuel form proposed in this study (i.e. BISO fuel with a UN kernel operating at high temperatures with relatively high packing fractions).

In addition to UN kernels and radial enrichment zoning, optimisation of the higher power output core configuration focused on:

1. Increasing the core size. This allowed an increase in power density to 10.7 MW/m^3 compared with the nominal OPUS design, which has a power density of 4.3 MW/m^3 .
2. Investigating the impact of changing the aspect ratio of the core (e.g. taller core configurations).
3. Increasing the number of fuel elements and reducing the coolant channel size, whilst keeping the total coolant channel cross section within the core constant.
4. Modifying the coolant gas composition from 85 g/mol He-Xe to 20 g/mol.

As will be detailed, whilst in principle items 2 and 4 above can allow for significant improvements in the power density, the inevitable engineering trade-offs associated with gas-cooled reactors are ultimately too penalising to make these options viable. Option 3 (resulting in the design iteration referred to as JANUS) successfully resulted in a much higher power density than the nominal OPUS core (4.3 MW/m^3 vs 26.5 MW/m^3) without unacceptable engineering trade-offs.

Regarding option 4, a reduction in coolant atomic mass from 85 g/mol to 20 g/mol permitted a 34% reduction in core volume. However, the higher helium content will adversely impact the volume and/or mass of turbo-machinery required to convert the thermal heat to electricity (El-Genk and Tournier, 2006). Considering the reactor core is a relatively small fraction of the overall energy system mass (around one-third of total mass (Cliquet et al.,

2011)), the 34% reduction in core volume and mass was not judged by the authors to be significant enough to overcome the much larger turbo-machinery volume and mass needed, which will prohibitively add to the launch mass.

3.1. Increasing core size and implementing radial enrichment zoning

Using the nominal OPUS core design as a starting point, the core thermal power was increased to 3 MWth and the core size increased in both radial and axial directions. In addition, the enrichment was modified such that there was sufficient excess reactivity at beginning of life (BOL) of around 3000 pcm to allow for 2000 Effective Full Power Days (EFPD) of operation, outlined in Table 2. Furthermore, radial enrichments were varied manually in order to flatten the power shape and therefore reduce peak operating temperature. The thermal dimensioning tool outlined in Section 2.3 was then used to estimate the peak operating temperature for a core with a 880 K core inlet temperature and 1300 K core outlet coolant temperature and to ensure the radial enrichment zoning was sufficient to maintain peak fuel operating temperatures below 1900 K.

To meet the criteria regarding excess reactivity at BOL and peak fuel temperatures, only 4 radial enrichments (ranging from 30 wt.% in the core centre to 60 wt.% on the core periphery, equivalent to a volume average enrichment of 50 wt.%) were necessary, as outlined in Table 6. The final core design had a power density of 10.7 MW/m³ (compared with 4.3 MW/m³ for the nominal OPUS design).

Table 6. Radial enrichment zones, starting from the centre of the core, for the core configuration with a radius of 35.5 cm and hexagonal fuel element pitch of 3 cm.

Radial zone number	²³⁵ U enrichment	Proportion of core at this enrichment
Zone 1	30 wt.%	10%
Zone 2	40 wt.%	30%
Zone 3	50 wt.%	10%
Zone 4	60 wt.%	50%

3.2. Decreasing the core aspect ratio

A number of cores were designed with aspect ratios ranging from 0.3 up to 1.5, where the aspect ratio is defined to be $2R_c/H$, where H is the active core height and R_c is the active core radius. The core configuration with an aspect ratio of 1.0 is the same as that outlined in Section 3.1. For each core model, radial enrichment zoning, as well as UN BISO fuel were used along with an the requirement for an excess reactivity of 3000 pcm at BOL. Furthermore, the fuel element geometry was the same as the nominal OPUS fuel design (3 cm hexagonal pitch with a 1 cm diameter central coolant channel) but with varying axial heights. For each case, the core volume was varied until the predicted peak temperature was around 1850 K, which is less than the peak operating temperature limit of 1900 K.

Table 7 shows the predicted peak operating temperatures along with the total core volumes and predicted pressure drops across the core. The results show that a factor of two

Table 7. Impact of adjusting core aspect ratio on peak temperature, power density and core pressure drop

Aspect Ratio	Active Height (m)	Core Volume (m ³)	Peak Fuel Temperature (K)	Core Pressure Drop (MPa)	Power Density (MW/m ³)
0.30	1.19	0.12	1840 K	1.240	25.2
0.50	0.94	0.16	1800 K	0.365	18.2
0.70	0.80	0.19	1840 K	0.175	15.5
1.00	0.71	0.28	1830 K	0.064	10.7
1.20	0.65	0.32	1820 K	0.042	9.5
1.50	0.61	0.40	1820 K	0.022	7.5

increase in power density is achievable for a highly elongated core (i.e. aspect ratio of 0.3). However, the pressure drop across the core is over 1 MPa, similar to the operating pressure of the OPUS core. Such a design would require a significant increase in compressor size and additional structural support, probably resulting in no overall mass or volume savings, noting that usually only around a third of the power system mass is the reactor core itself (Cliquet et al., 2011).

3.3. Increasing the number of fuel elements and reducing the coolant channel size

A number of different sized cores were modelled using ERANOS ranging from a relative core volume of 0.3 up to 1.5. For each core:

- the total power output was set to 3 MWth;
- radial enrichment zoning was used to limit peak to average power production; and
- an excess reactivity target at BOL of 3000 pcm was applied to ensure sufficient margin for at least 2000 EFPD.

The thermal dimensioning tool was then used to assess how large each fuel element would need to be in to keep the peak fuel temperature within the given limit.

As the fuel element hexagonal pitch is decreased, which results in the heat transfer path between the fuel and coolant reducing and a corresponding improvement in heat transfer. The core volume can therefore be reduced, as shown in Table 8. However, the reduction in coolant channel diameter and fuel element pitch results in an increase in pressure drop across the reactor core leading to the requirement for a larger and therefore heavier gas compressor.

Assuming a system pressure of 1.4 MPa, a relative surface roughness 2 μm and a combined K-factor of 1.5, estimates for the pressure drop (Incropera and DeWitt, 1990) across the core have been calculated and are given in Table 8. Although large for the smaller core designs, the pressure drop across the turbine is likely to be much higher (we estimate using engineering judgment this to be around half the core system pressure (i.e. 0.7 MPa)). The core configurations summarised in Table 8 were based on maintaining a core aspect ratio of 1.0 (i.e. core height = core diameter); fuel elements with equivalent coolant channel to

fuel matrix area ratios; and employing the thermal dimensioning tool outlined in Section 2.3 with a target peak fuel temperature of approximately 1850 K.

As shown in Table 8, reducing fuel element pitch will lead to an increase in core pressure drop and therefore an increase in compressor size and volume in order to pump the coolant through a more restricted core. However, for all but the smallest fuel element design, the increase in compressor mass and volume required to increase reactor inlet pressure head will not be significant and will potentially be offset by the large reduction in core volume as a result of improved heat transfer. Therefore, an increase in the number and a reduction in individual coolant channel surface area is considered to be very effective at increasing core power density.

To ensure the use of homogeneous ERANOS models for cores significantly larger than the nominal OPUS design was still broadly valid, a comparison was performed on one of the larger core configurations, namely the core with a radius of 35.5 cm and 71.0 cm active height outlined in Table 8. The discrepancy between the homogeneous ERANOS model vs the SERPENT model for this larger core was found to be 333 ± 1 pcm, which is similar to the 288 pcm discrepancy observed when modelling the smaller nominal OPUS design (see Section 2.2).

Table 8. Effect of changing fuel element geometry on power density and core pressure drop when maintaining a core aspect ratio of 1.0 (i.e. core height = core diameter)

Coolant channel diameter (mm)	Distance between flats of hexagonal fuel element (mm)	Active core height (cm)	Active core radius (cm)	Power density (MW/m ³)	Peak fuel temperature (K)	Core pressure drop (MPa)
7.1	21.5	49.2	24.6	32.0	1856	0.27
7.4	22.3	54.2	27.1	24.0	1813	0.19
8.5	25.7	58.4	29.2	19.2	1831	0.14
9.0	27.2	62.0	31.0	16.0	1819	0.11
10.0	30.0	71.0	35.5	10.7	1826	0.06
12.4	37.2	84.1	42.1	6.42	1838	0.03

We assume a limit of 0.20 MPa for the pressure drop limit across the core so that the pressure drop across the core remains small compared with the pressure drop expected across the rest of the direct cycle loop. Hence the optimal core configuration from Table 8 is the iteration with a coolant channel diameter of 7.4 mm and a power density of 24.0 MW/m³. This iteration is referred to as the JANUS concept.

Note that for the JANUS concept, the minimum width region is 11.15 mm - 3.7 mm = 7.45 mm. Given the size of the particles (1 mm), the minimum width of the fuelled region is not much larger than the size of the particles (7.45 particles) means that the particles are not completely free to distribute in a random fashion. Thus, some of the particles will likely be distributed as quasi-crystals, and a significant fraction of particles will likely be touching each other. Hence, there is a significant risk of cracking and future work would need to investigate the likelihood of fuel failure, potentially necessitating irradiation trials. Further optimisation of the fuel configuration may be required to ensure a fuel failure fraction that is acceptable for the aims of the JANUS concept (noting earlier discussion on acceptability of higher failure fracture compared to conventional TRISO particles for this particular space

reactor concept).

3.4. Summary of optimisation choices and JANUS core characteristics

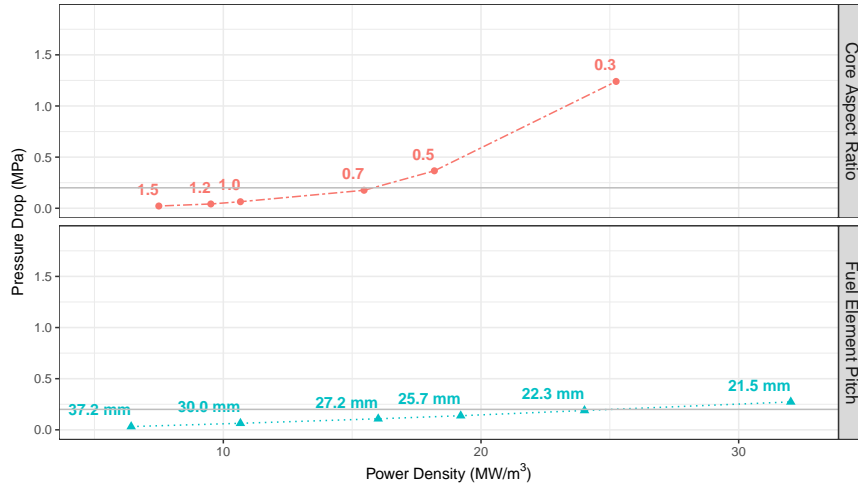


Fig. 4. The impact on pressure drop for two core design configurations as a function of power density, including the 0.2 MPa core pressure drop limit imposed on the core iterations

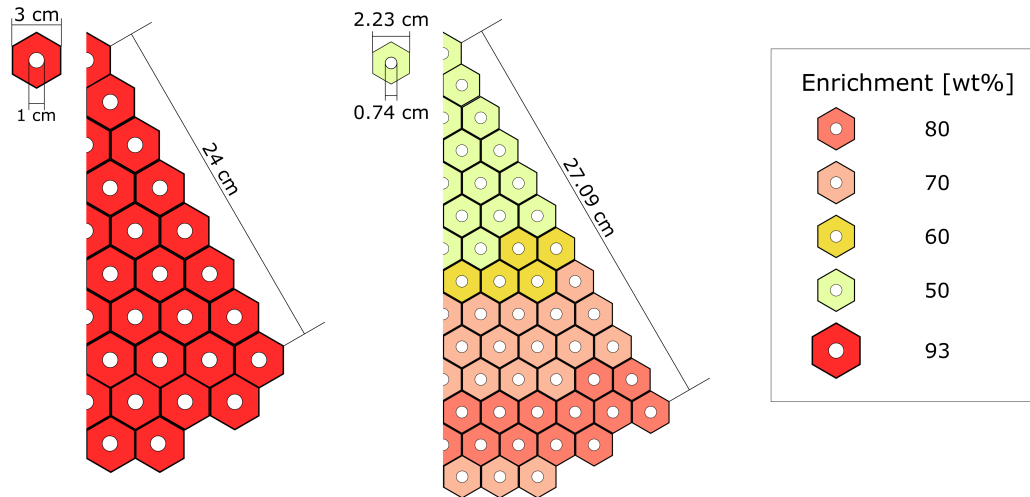


Fig. 5. Comparison of the nominal OPUS core and the JANUS variant developed in this study

Simply increasing the core size and employing radial enrichment heterogeneity allows for an increase in power density from 4.3 MW/m³ (the nominal OPUS design) to 10.7 MW/m³, noting there will be a drawback associated with the larger coolant inventory and therefore larger turbo-machinery. For a given pressure drop sacrifice, reducing the fuel element pitch

Table 9. Nominal OPUS core and the JANUS core key parameters

Parameter	Nominal OPUS Core	JANUS Core
Thermal power	0.370 MWth	3 MWth
Electrical power	0.100 MWe	0.811 MWe
Active core diameter	48 cm	54.2 cm
Active core height	48 cm	54.2 cm
Mean ^{235}U enrichment	93 wt.%	68 wt.%
Fuel element pitch (across flats)	3 cm	2.23 cm
Coolant channel diameter	1cm	0.74 cm
Fuel elements in core	252	418
Fuel form	Graphite matrix containing 45% BISO fuel particles by volume	
Kernel type	UO_2	UN
Coolant type	85 g/mol He-Xe	85 g/mol He-Xe
Coolant flow rate	3.6 kg/s	29.2 kg/s
Radial reflector thickness	8 cm	8 cm
Axial reflector	8 cm	8 cm
Number of radial enrichment zones	1	5
Power density	4.3 MW/m ³	24 MW/m ³

is far more effective at reducing core mass and volume as shown in Figure 4. We assume a limit of 0.20 MPa for the pressure drop limit across the core so that the pressure drop across the core remains small compared with the pressure drop expected across the rest of the direct cycle loop. Elongating the core allows for a power density of approximately 16 MW/m³, whilst ensuring the pressure drop is below 0.20 MPa. Conversely, reducing the fuel element pitch (whilst keeping the total coolant channel cross sectional area in the core constant), allows for a power density of 24 MW/m³.

Table 9 gives a comparison of the nominal OPUS core parameters (Raepsaet and Pascal, 2007, Likhov, 2009) and the JANUS core parameters. For completeness, a comparison of the two cores is included in Figure 5.

As a further comparison, the flux spectrum from the JANUS heterogeneous SERPENT model, taken across the whole-core including the beryllium reflector was compared with a typical SFR spectrum (Sciora et al., 2011) and PWR spectrum (SERPENT, 2020) as shown in Figure 6. The PWR spectrum is based on a VVER-440 assembly design (SERPENT, 2020). Note that the energy integrated flux has been scaled in all cases to a maximum of 1.0. Figure 6 shows that the JANUS core exhibits a spectrum somewhere between the PWR and SFR cases modelled since, whilst a beryllium reflector is employed and there is a significant amount of graphite, this is offset by the high enrichment, the very high packing fraction of the BISO particles in the fuel and the use of a non-moderating coolant.

Finally, the impact of employing 95% vs 100% enriched fuel ^{15}N was investigated for

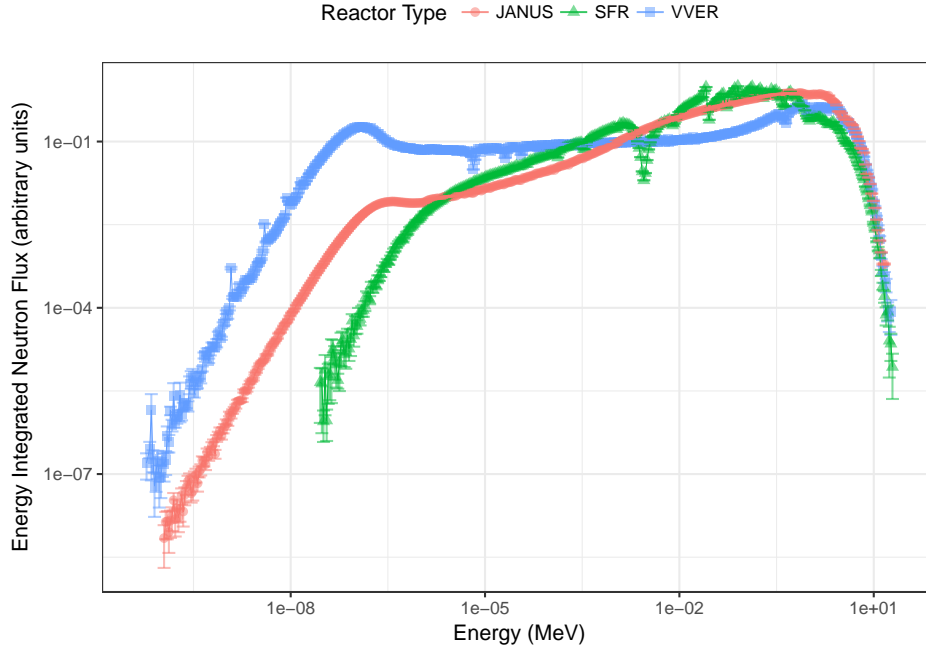


Fig. 6. Comparison of flux spectrum between JANUS, SFR and PWR (VVER) SERPENT models.

the JANUS model. Starting with the SERPENT heterogeneous model and performing the calculation at beginning-of-life, this showed a reactivity penalty of 79.2 ± 8.6 pcm.

4. Future Work

Whilst the design constraints employed here are consistent with those in the literature, it is important to note that peak temperatures of 1900 K, even for coated particle fuel, is high and operational experience of particles operating at such temperatures (even if the peak temperatures close to 1900 K are only sustained for a portion of the reactor’s life) is only $\sim 10^2$ hours. Furthermore, whilst there is experience with high packing fractions, the use of thin fuel elements proposed in the JANUS design may result in some of the particles distributed as quasi-crystals and therefore they may be in close contact, resulting in elevated failure probabilities. Hence, even though higher failure fracture than conventional HTRs can be tolerated for an unmanned mission, it would be important to ensure that failure rates are not onerously high; thereby allowing for large ingress of chemically aggressive fission products escaping the core and damaging system components. Future work would need to consider the trade-off between high power densities, high packing fractions and fuel failure rates. This would potentially necessitate irradiation trials for the fuel configuration proposed.

5. Conclusions

Many current and published gas-cooled space reactor designs operate at relatively low power output and low power densities, such as the CEA’s OPUS concept, which employs

UO₂ BISO fuel with a He-Xe gas coolant and has a power output of 0.100 MWe, with a power density of 4.3 MW/m³. However, such low power outputs make these cores unsuitable for future space applications, including cargo support for a manned mission to Mars and outer Solar System missions with large mission payloads. Hence, there is a desire to develop a space reactor with high power density (to minimise launch mass and volume) and high power output (around 1 MWe).

Starting from this published OPUS design, a gas-cooled space reactor concept, referred to as JANUS, has been developed at the conceptual level, that operates at a much higher power output (0.8 MWe) and significantly increased power density 24 MW/m³. The fuel form adopted in the JANUS concept is uranium nitride BISO fuel to help reduce demands on enrichment and provide greater flexibility in radial enrichment zoning. The optimisation route to develop a viable gas-cooled space reactor involved neutronic and thermally modelling the different core designs to ensure key criteria related to core-life (2000 EFPD) and peak fuel operating temperatures (1900 K) were obeyed. In addition, comparisons involving Monte Carlo neutronic calculations using SERPENT were used to validate the ERANOS calculation route adopted in this study. The discrepancies between ERANOS and SERPENT of around 500 pcm showed that the approach adopted in this study was sufficiently accurate for the purpose of scoping out viable core configurations as part of the optimisation route.

For thermal modelling, a simple yet robust thermal dimensioning tool has been developed as part of this study to ensure accurate but computationally efficient predictions on peak temperature so that the fuel could be expected to operate within its design constraints. The thermal dimensioning tool was shown to accurately predict peak fuel temperatures in the original OPUS design, when compared with the results from the CEA's Cast3M finite element calculations, and greatly aided in the optimisation process when considering many core variants.

A key outcome of this study related to identifying the inherent challenges with increasing power density when employing a gas-coolant operating with a direct Brayton cycle. The use of a gas-coolant inherently limits the achievable power density and the mechanisms to improve heat transfer between the coolant and fuel (to ensure fuel operating temperature are below the 1900 K limit) often result in larger pressure drops across the core and/or greater demands on the turbo-machinery. This results in unacceptable increases in launch mass and volume. Nevertheless, adopting a new fuel element design, that reduced the heat transfer path between the fuel and coolant, and employing greater radial heterogeneity has resulted in a core design capable of meeting the design constraints.

Acknowledgements

This work was supported by the National Nuclear Laboratory's (NNL's) Innovation Research and Development fund. The authors would also like to gratefully acknowledge input received from Thomas Bennett (NNL), Bruno Merk (University of Liverpool) and Richard Stainsby (Wood plc).

References

- Bennett, G. L. (2002). Space nuclear power. In *Encyclopaedia of Physical Science and Technology*, pages 537–553. Academic Press, New York, 3 edition.
- Botts, T. et al. (1984). A bi-model reactor for high and low space power. In *1st Symposium on Space Nuclear Power Systems*, Alburquerque, USA.
- Brandon, D. and Sapir, J. (1986). Criticality-safety analyses of compacted and water-flooded sp-100 reactors. In *ANS Topical Meeting on Reactor Physics and Safety*, Saratoga Springs, New York, USA.
- Briggs, M., Gibson, M., and Sanzi, J. (2018). Electrically Heated Testing of the Kilowatt Reactor Using Stirling Technology (KRUSTY) Experiment Using a Depleted Uranium Core. Technical report, National Aeronautics and Space Administration. NASA/TM- 018-219702.
- Carre, F. et al. (1987). Status of cea design and simulation studies of a 200 kwe turboelectric space power system. In *4th Symposium on Space Nuclear Power Systems*, Alburquerque, USA.
- Carslaw, H. S. (1959). *Conduction of heat in solids, second edition*. Oxford University Press.
- Cliquet, E. et al. (2011). Preliminary study of a 100 kWe space reactor concept for exploration missions. Nuclear and Emerging Technologies for Space.
- Da Cruz, D., Hogenbirk, A., Bosq, J., Rimpault, G., Prulhiere, G., Morris, P., and Pelloni, S. (2006). Neutronic benchmark on the 2400 mw gas-cooled fast reactor design. in *Proc. of PHYSOR-2006*.
- Delaplace, J. (1987). Space electronuclear generators studies in france. *Acta Astonautica*, 15:941–944.
- Demuth, S. (2003). Sp100 space reactor design. *Progress in Nuclear Energy*, 42:323–359.
- El-Genk, M. and Tournier, J. (2006). Selection of noble gas binary mixtures for brayton space nuclear power systems. In *4th International Energy Conversion Engineering conference and exhibit*, San Diego, California.
- El-Genk, M. S. and Tournier, J.-M. P. (2004). SAIRS – Scalable Amtec Integrated Reactor space power System. *Progress in Nuclear Energy*, 45(1):25–69.
- European Science Foundation (2014). Megawatt highly efficient technologies for space power and propulsion systems for long-duration exploration missions - project final report. Technical report, European Science Foundation.
- Ganguly, C. (1993). Sol-gel microsphere pelletization: A powder-free advanced process for fabrication of ceramic nuclear fuel pellets. *Bulletin of Materials Science*, 16(6):509–522.
- Guerin, Y. (2012). Fuel Performance of Fast Spectrum Oxide Fuel. In Konings, R., Allen, T., Stoller, R., and Yamanaka, S., editors, *Comprehensive Nuclear Materials*, chapter 2.21, pages 547–578. Elsevier Ltd., Waltham.
- Gulden, T. D. et al. (1977). Coated particle fuels. *Nuclear Technology*, 35.
- Howard, R., Price, M., and Shepherd, E. (1978). Summary and evaluation of the achievements of the dragon project and its contribution to the development of the high temperature reactor. Technical report, UKAEA.
- IAEA (2008). Thermophysical properties of materials for nuclear engineering: a tutorial and collection of data. Technical report, IAEA.
- IAEA (2010). High temperature gas cooled reactor fuels and materials. Technical report, IAEA. IAEA-TECDOC-1645.
- IAEA (2019). Waste from innovative types of reactors and fuel cycles: a preliminary study. Technical report. NW-T-1.7.
- Incropera, F. and DeWitt, D. (1990). *Introduction to heat transfer*. John Wiley and Sons.
- IRSN (2015). Review of generation iv nuclear energy systems. Technical report, IRSN.
- Khandaq, M. F., Harto, A. W., and Agung, A. (2020). Conceptual core design study for indonesian space reactor (isr). *Progress in Nuclear Energy*, 118:103109.
- Kingrey, K. I. (2003). Fuel summary for peach bottom unit 1 high- temperature gas-cooled reactor cores 1 and 2. Technical report, INEEL.
- Launius, R. (2008). Powering space exploration: Us space nuclear power, public perceptions, and outer planetary probes. In *6th International Energy Conversion Engineering Conference (IECEC)*, page 5638.
- Ledergerber, G., Ingold, F., Stratton, R. W., Alder, H.-P., Prunier, C., Warin, D., and Bauer, M. (1996).

- Preparation of transuranium fuel and target materials for the transmutation of actinides by gel coconversion. *Nuclear Technology*, 114(2):194–204.
- Ledergerber, G., Kopajtic, Z., Ingold, F., and Stratton, R. (1992). Preparation of uranium nitride in the form of microspheres. *Journal of nuclear materials*, 188:28–35.
- Lee, H. C., Lim, H. S., Han, T. Y., and Čerba, Š. (2015). A neutronic feasibility study on a small leu fueled reactor for space applications. *Annals of Nuclear Energy*, 77:35–46.
- Leppanen, J. (2007). *Development of a new monte carlo reactor physics code*. PhD thesis, Helsinki University of Technology, Helsinki, Finland.
- Lokhov, A. (2009). Advances in design and modeling of the reactor core of opus. In *Nuclear and emerging technologies for space 2009*, Atlanta, USA.
- Nam, S. H., Venneri, P., Kim, Y., Chang, S. H., and Jeong, Y. H. (2016). Preliminary conceptual design of a new moderated reactor utilizing an leu fuel for space nuclear thermal propulsion. *Progress in Nuclear Energy*, 91:183–207.
- NASA (2004). Ion propulsion. Technical report, NASA. FS-2004-11-021-GRC.
- NASA (2005). Prometheus project - final report. Technical report, NASA.
- NEA (2000). The jef-2.2 nuclear data library. Technical report, OECD NEA.
- Noca, M. and Polk, J. (2002). Ion thruster and LFAs for outer planet exploration. In *AAF 6th International Symposium on Propulsion for Space Transportation of the XXXIst Century*, Versailles, France.
- OSNET (2014). Russia advances development of nuclear powered spacecraft. <http://osnetdaily.com/2014/01/russia-advances-development-of-nuclear-powered-spacecraft>. Accessed: 2016-03-31.
- Pascal, S. (2010). Coupled 1d thermohydraulic - 3d thermomechanical study of a space nuclear reactor. In *4th European Conference on computational mechanics*, Paris, France.
- Peakman, A., Hodgson, Z., and Merk, B. (2018). Advanced micro-reactor concepts. *Progress in Nuclear Energy*, 107:61 – 70.
- Petti, D. et al. (2012). TRISO-Coated Particle Fuel Performance. In Konings, R., Allen, T., Stoller, R., and Yamanaka, S., editors, *Comprehensive Nuclear Materials*, chapter 3.07, pages 151–213. Elsevier Ltd., Waltham.
- Petti, D. A. (2007). Detailed PIRT Submittal by the INEEL Panel Member Appendix H.1. Technical report, NRC.
- Petti, D. A. and Maki, J. (2005). The Challenges Associated with High Burnup and High Temperature for UO₂ TRISO Coated Particle Fuel. Technical report, INL.
- Pierce, B. (1984). Gas cooled reactor concepts for space application. In *1st Symposium on Space Nuclear Power Systems*, Alburquerque, USA.
- Polansky, G. and Houts, M. (1995). A preliminary investigation of the topaz ii reactor as a lunar surface power supply. Technical report, Sandia National Laboratory.
- Ponya, P. and Czifrus, S. (2017). Core optimisation issues of MOX Fueled ALLEGRO reactor. *Annals of Nuclear Energy*, 108:188 – 197.
- Poston, D. (2000). The Heatpipe-Operated Mars Exploration Reactor (HOMER). Technical report, Los Alamos Natl. Lab. LA-UR-00-5269.
- Raepsaet, X. and Pascal, S. (2007). Neutronic and mechanical design of the reactor core of the opus system. In *ICAPP 2007*, Nice, France.
- Ray, S., Lahoda, E., and Franceschini, F. (2012). Assessment of different materials for meeting the requirement of future fuel designs. In *2012 Reactor Fuel Performance Meeting*, volume 115.
- Reid, R. et al. (2007). Heat transfer and pressure drop in concentric annular flows of binary inert gas mixtures. Technical report, NASA.
- Rimpault, G. and Grimstone, M. (2002). The eranos code and data system for fast reactor neutronic analyses. In *PHYSOR 2002*, Seoul, South Korea.
- Sawa, K. (2012). TRISO Fuel Production. In Konings, R., Allen, T., Stoller, R., and Yamanaka, S., editors, *Comprehensive Nuclear Materials*, chapter 3.06, pages 143–149. Elsevier Ltd., Waltham.
- Sciora, P., Blanchet, D., Buiron, L., Fontaine, B., Vanier, M., Varaine, F., Venard, C., Massara, S., Scholer, A.-C., and Verrier, D. (2011). Low void effect core design applied on 2400 MWth SFR reactor. In

- International Congress on Advances in Nuclear Power Plants (ICAPP)*, volume 595.
- SERPENT (2020). 2D VVER-440 fuel assembly geometry. http://serpent.vtt.fi/mediawiki/index.php/2D_VVER-440_fuel_assembly_geometry. Accessed: 2020-01-31.
- Simon, R. A. and Capp, P. D. (2002). Operating experience with the dragon high temperature reactor experiment. Technical report, IAEA.
- Verfondern, K. (2012). TRISO Fuel Performance Modeling and Simulation. In Konings, R., Allen, T., Stoller, R., and Yamanaka, S., editors, *Comprehensive Nuclear Materials*, chapter 3.24, pages 755–788. Elsevier Ltd., Waltham.
- WNA (2020). Nuclear reactors and radioisotopes for space. <https://www.world-nuclear.org/information-library/non-power-nuclear-applications/transport/nuclear-reactors-for-space.aspx>. Accessed: 2020-01-03.